Active Silicon Photonic Device Performance after ^{60}Co Gamma Radiation

Galen Hoffman, Michael Gehl, Nicholas Martinez, Douglas Trotter, Andrew Starbuck, Andrew Pomerene, Christina Dallo, Dana Hood, Paul Dodd, Scot Swanson, Christopher Long, Christopher DeRose, and Anthony Lentine
Sandia National Laboratories
Albuquerque, NM 87123
Email: ghoffma@sandia.gov

***Abstract*—In this work, we test Si vertical junction disk modulators and waveguide-integrated Ge PIN photodiodes to see how the key performance metrics are affected by ^{60}Co gamma radiation (total ionizing dose), a common proxy for simulating a mix of high energy ion particle flux. It is found that reverse bias dark current increases significantly for both devices after 1 Mrad exposure. Whereas the bandwidth of the Si disk modulator decreases by 6.5 % to 16.6 GHz after 1 Mrad dose, the bandwidth of the Ge PIN photodiode is unaffected and remained close to 40 GHz to within the uncertainty of the measurement.**

Keywords—electrooptic modulators; photodetectors; photodiodes; silicon photonics; integrated optoelectronics; integrated optics; gamma-ray effects; total ionizing dose; space radiation; optical fiber communication

I. Introduction

Silicon photonics (SiP) has emerged as the leading technology for optical communications due to its low power consumption on the order of femtojoules per bit [1], high bandwidth using wavelength division multiplexing (WDM) [2],[3] and fabrication methods compatible with CMOS circuits [4]. Compact, lightweight and inexpensive highly integrated SiP transceivers have been used for long haul [5] and metro telecommunications [6] as well as in datacenters [7],[8]. Photonic devices have also been proposed for use in harsh environments under elevated temperatures and high radiation levels.

Space applications represent a compelling use case for high bandwidth and low power SiP circuits. Specifically, focal plane arrays (FPA) are used to remotely monitor targets on and off the earth using large arrays of light-sensing pixels [9]. For instance, the Kepler space telescope focal plane array is composed of 96 million total pixels each operating at a 10 Hz data (frame) rate and dissipating ~100 W for the detector power, control and readout systems [10]. If the array size or frame rate were increased or compound (multispectral) array pixels were used this could easily lead to a dramatic increase in the array's power usage above a kilowatt. Previously, a WDM SiP-driven photonic FPA backplane was proposed to enable much higher data transfer rates and an order of magnitude power reduction [11],[12]. This SiP backplane would also have the added advantages of lower weight and the elimination of electromagnetic interference (EMI).

A key question is the tolerance of the electro-optical devices such as vertical cavity surface emitting lasers (VCSELs) [13], Ge photodiodes [14] – [16] and Si disk or ring diode modulators [1],[17] – [21], to the radiation extremes experienced in space and specifically, a low earth orbit environment. This environment is characterized by high fluxes of ionized particles from the solar wind, solar flares, cosmic rays and particles trapped in the Van Allen belts [22],[23]. The particles of interest have energy from below 1 MeV up to 100 MeV and can cause both ionization and displacement damage within the semiconductor devices [24]. For radiation hardness testing, rather than attempting to replicate the exact environment (i.e. a distribution of high energy ionized atomic nuclei), often proxies are used which are known to have similar ionizing effects such as gamma radiation from a 60Co source which emits at 1.1 & 1.3 MeV [23],[24]. Previous works addressing the operation of photonic devices in harsh environments have focused on VCSELs [25] – [27], integrated Si MZMs and Ge PIN photodiodes [28] under gamma irradiation, Si disk modulators at cryogenic temperatures [29],[30] and Ge avalanche photodiodes (APDs) under proton and gamma irradiation [31]. In this work, we report on the effect of gamma radiation from a 60Co source up to 1 Mrad (10 kGy) TID on the performance parameters of waveguide-integrated Ge PIN photodiodes and vertical junction Si disk modulators.

II. Experimental

A. Device Design and Fabrication

These devices were fabricated using Sandia's CMOS-compatible silicon photonics process. The fabrication details for the Si disk vertical junction modulators [19] and the waveguide-integrated Ge PIN photodiodes 14] have been described previously [4]. Fig. 1 shows the structure, minus the oxide over cladding, for the Ge PIN and Fig. 2 shows the structure for the disk modulator.

B. Sample Irradiation

The purpose of irradiation was to determine gamma TID effects on device performance parameters. We used a 60Co source with about ~130 rad (Si)/s dose rate. Temperature was controlled by blowing air to an approximate temperature of 24

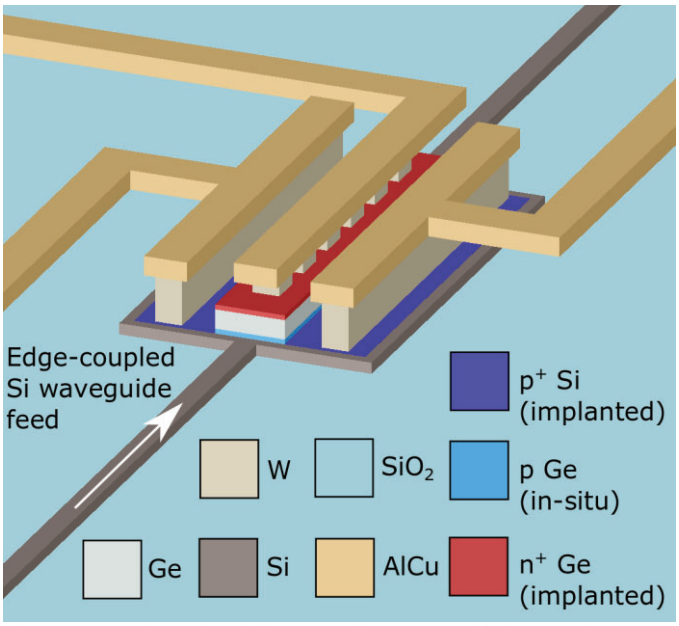

Fig. 1. 3D schematic of the 8 μm long waveguide-integrated Ge PIN photodiode with solid contacts to Si and a 6-segment contact to the Ge.

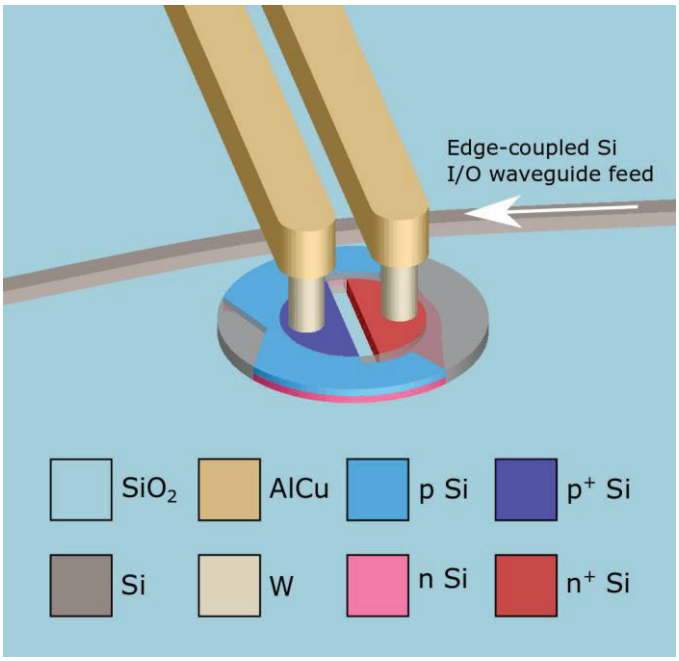

Fig. 2. 3D schematic of the finished Si vertical junction microdisk. The n- and p-doped regions are shifted towards the left side of the disk, leading to a shorter mean path length for holes versus electrons. The undoped disk material is slightly transparent to show the extension of the n-doped region underneath. The waveguide feed curves slightly around the disk to provide a longer coupler length.

deg. C during irradiation. Devices were biased at 1 V reverse bias through Au wirebonds to a sub-miniature push-on (SMP) and connector which was mounted to a Cu sample holder along with the sample under test with epoxy. The soft Au wirebonds could easily be completely removed after irradiation to ensure good contact with RF probes for post measurement. For each sample gamma irradiation was done in steps, between which optoelectronic measurements were made, ensuring that the sample received a certain cumulative dose after each step. The post irradiation measurements after each dose step were started within 1 hour after the dose was received and no more than 8 hours elapsed between the receipt of the first dose and the final measurement. We irradiated up to total cumulative doses of 1 Mrad as a worst-case estimate for a shielded satellite on a ~ 5 year mission in low earth orbit [30].

C. Electro-optic Characterization

Heterodyne interference between two lasers (one tunable) was used to produce a beat note (difference frequency) to probe the RF response of the Ge PIN photodiodes. Each laser was equipped with independent polarization controllers which were set to transverse electric (TE, i.e. the electric field is oriented parallel to the plane of the test sample chip) with only the corresponding laser on to ensure that both lasers were at the same polarization. The lasers were combined in a 3dB splitter one output of which was directed through a cleaved single mode fiber (SMF) and butt coupled to the edge of the test sample. The test sample was mounted to a Cu mount with Ag epoxy, which itself was attached to a thermoelectric cooler (TEC) that is rated up to 200 °C operation. An Infinity GSG100 probe from Cascade Microtech was used to probe the device for both DC and RF measurements. The probe was connected through a bias tee at 1 V reverse bias to an Agilent N1913A power meter with 8487D power sensor. For DC measurements the GSG probe was connected directly to the current-voltage source, an Agilent B1500A semiconductor analyzer with a high-resolution source-measure unit. To obtain an RF response spectrum, the wavelength of the tunable laser was swept, and the power meter's value was recorded at each wavelength. The RF response of the device was corrected for the known response of the bias tee, cable and probe which were measured with an Agilent 50 GHz vector network analyzer (VNA).

For the disk modulators Samples were temperature controlled, mounted, DC biased and probed in the same manner as with the Ge PIN photodiodes. In this case however only a single tunable laser source was used. The polarization was set to TE. A cleaved SMF was used to outcouple light from the chip which was then connected to a C-band EDFA and tunable bandpass filter.

RF characterization was done using a VNA to probe the response of the modulator from the behavior of S21. The VNA is used to calibrate the response of the probes, cable, DC block, and bias tee. The response of photodetector was also calibrated out of the measured S21 and was determined using heterodyne interference.

A Centellax TG1B1 BERT and TG1C1 10 GHz clock generator are used to generate a 2E-7 pseudo-random bit sequence (PRBS), which is applied to the device through a bias tee at 2 V reverse bias. The output of the tunable filter is connected to a variable optical attenuator (VOA) which is used to vary the received power for BERT. A 12 GHz Optilab LR-12-M with 500 Ω transimpedance gain receives the light signal and feeds through a DC block to a 20 GHz oscilloscope (for eye

diagram acquisition) or to the BERT module for testing. Consistency between successive tests of either different temperatures or total radiation doses is assured by monitoring the fiber-to-chip coupling insertion loss at an off-resonance wavelength in the C-band at 1540 nm. Changes to the insertion loss were compensated by changing the attenuation of the laser to ensure that the same power is incident on the device. DC bias and BERT signal amplitude were also kept the same for room temperature pre-measurements and for irradiated post-measurements. The optical carrier wavelength and tunable bandpass filter were optimized to ensure open and symmetric eye diagrams before BERT was performed.

III. Results

A. Ge PIN Photodiode

The DC IV curves at 0 and 1 Mrad cumulative gamma dose were obtained. A compliance limit on the current magnitude was set to 100 µA to prevent device failure. A 1 Mrad (Si) gamma dose increases the dark current, here by factor of 1.45 at a 1 V reverse bias, which is shown in Fig. 3 (the compliance limit for this test was set to 50 µA).

The responsivity of the photodiodes was also measured. The bias on the diode was set to 1 V reverse bias. For this a single -10 dBm output laser with a SMF butt-coupled to the chip edge was used. Fiber alignment was accomplished by maximizing the photocurrent at a 1500 nm laser wavelength, resulting in a final photocurrent of about 70 µA. The laser wavelength was scanned from 1500 to 1635 nm and the current was recorded at each of the data points. The aligned photocurrent after the wavelength scan was validated to be within 100 nA of the original value, otherwise the fiber was realigned and the measurement repeated. This ensures that fiber coupling instability does not skew the results.

Responsivity is a measure of collected carrier current normalized to optical power incident on the device. Collected carrier current was calculated by subtracting the dark current at 1 V reverse bias from the measured photo current. Incident optical power was estimated first by calculating the spectral insertion loss of a straight through waveguide and taking the square root of the loss (halving in dB scale) to obtain the insertion loss for 1 end facet plus bus waveguide (the photodiodes are in the center of the chip). The optical power incident on the device is calculated by subtracting the single facet plus half-length waveguide insertion loss from the laser power. This calibration procedure was repeated at each cumulative gamma dose to account for changes in coupling or waveguide loss.

The device used for the radiation test had a responsivity of about 0.29 A/W at 22 °C before irradiation and an almost unchanged responsivity of 0.28 A/W after a 500 krad dose. After a 1 Mrad total dose however the responsivity at 1500 nm increased up to 0.34 A/W.

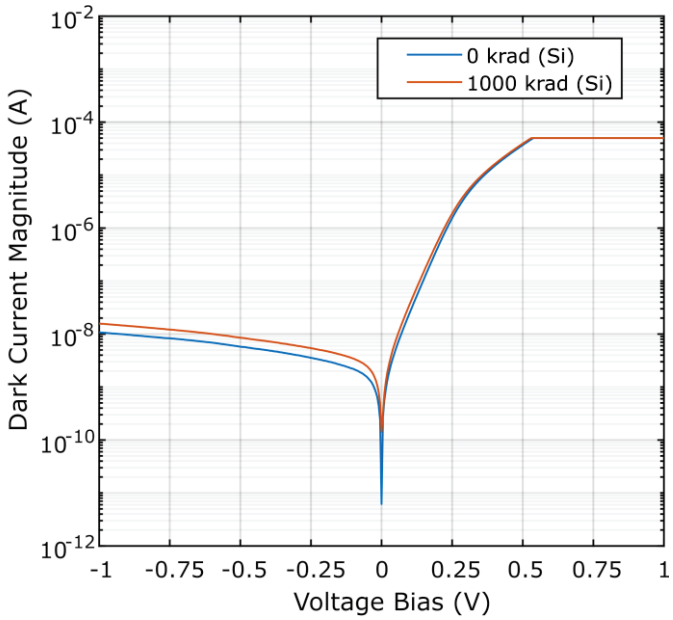

Fig. 3. Dark I-V characteristic for the 8 µm long Ge PIN photodiode under different conditions. Mount temperature is set at 20 °C with and without 1 Mrad ^{60}Co gamma irradiation. For a 1 V reverse bias the dark current increases by a factor of 1.45.

The spectral responsivity curves were normalized to the responsivity at 1500 nm and plotted in Fig. 4. No horizontal shifts are observed for increasing levels of gamma irradiation up to 1 Mrad.

The bandwidth of the Ge PIN photodiodes was characterized using heterodyne interference. After data collection the spectrum was shifted so that the peak is at 0 Hz and the bias tee, RF cable and probe were calibrated out of the measurement using a VNA. The resulting spectrum was fit to a simple lumped first order low pass filter RC model to obtain the 3dB bandwidth. The model function is $T(f) = a/(1 + (f/f_{3dB})^2)$, where T is the spectral power response, a is a constant, f is the frequency and f_{3dB} is the 3dB bandwidth. For both the gamma radiation test, 10 consecutive TE polarized heterodyne bandwidth scans were done at each gamma dose condition on the same sample to obtain statistics on measurement repeatability. This is due to the length of time the wavelength sweep takes during which the fiber can become misaligned and skew the results. For this reason, the spectrum on the negative side, which is acquired first, is used for the model fitting. Acquisitions with large noise events or poor fitting with $R^2 <$ 0.8 are removed from the analysis.

Fig. 5 shows the bandwidth results for different gamma radiation doses. No drop is seen for samples at 22 °C mount temperature that had been irradiated with 1 Mrad (Si) as the difference in means, ~0.5 GHz, is significantly smaller than the observed spread (inter-quartile range) of about 1 GHz. These results show that the Ge PIN photodiodes maintain their bandwidth and responsivity performance for large doses of ^{60}Co gamma irradiation up to 1 Mrad (Si).

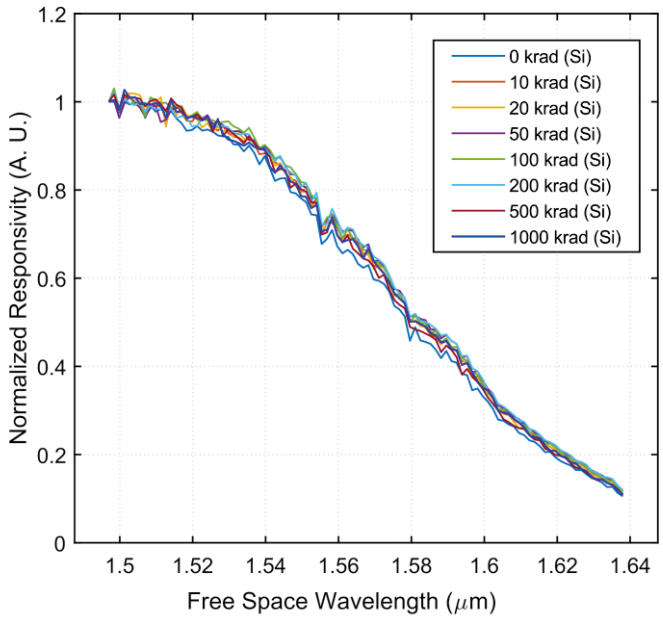

Fig. 4. Normalized responsivity versus wavelength for an 8 µm long waveguide-integrated Ge PIN photodetector at TE polarization. Laser power was -10 dBm. Mount temperature was set to 20 °C and 0 through 1 Mrad ^{60}Co cumulative gamma doses were tested. No horizontal shifts, indicating a bandgap shift, in the normalized responsivity spectra versus dose are observed.

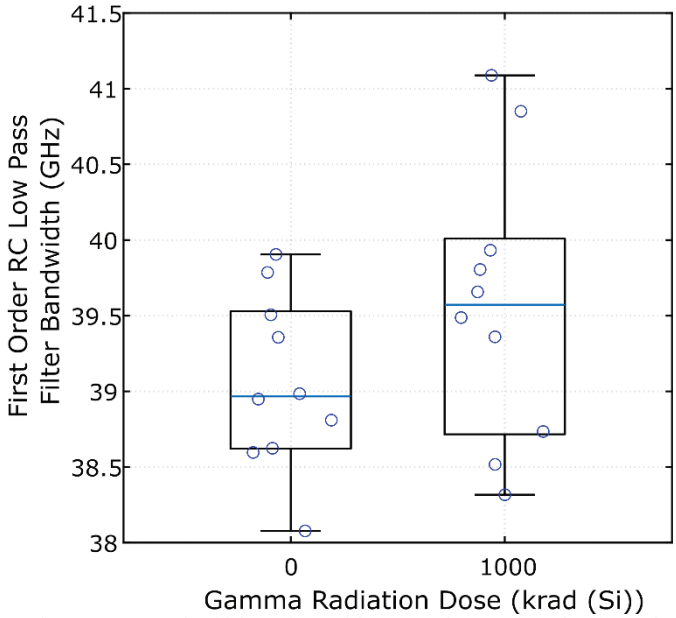

Fig. 5. Box and whisker plots with scatterplot overlay showing 3dB bandwidth for an 8 µm long waveguide-integrated Ge PIN photodiode at TE polarization, where the same device is measured 10 times in order to ensure repeatability. Boxes span first to third quartiles with blue median lines drawn. Whiskers extend out to minimum and maximum data points. mount temperature is set to 22 °C before and after a 1 Mrad ^{60}Co dose is applied. No significant change in the bandwidth of about 39 GHz is observed.

B. Vertical Junction Si Disk Modulator

DC IV curves were measured for the disk modulators under different gamma dose conditions. Fig. 6 shows that a 1 Mrad (Si) gamma radiation dose causes the reverse bias current to increase, here by a factor of ~70 which is proportionally much larger than that observed for the Ge photodiodes. No attendant built in voltage shift is observed.

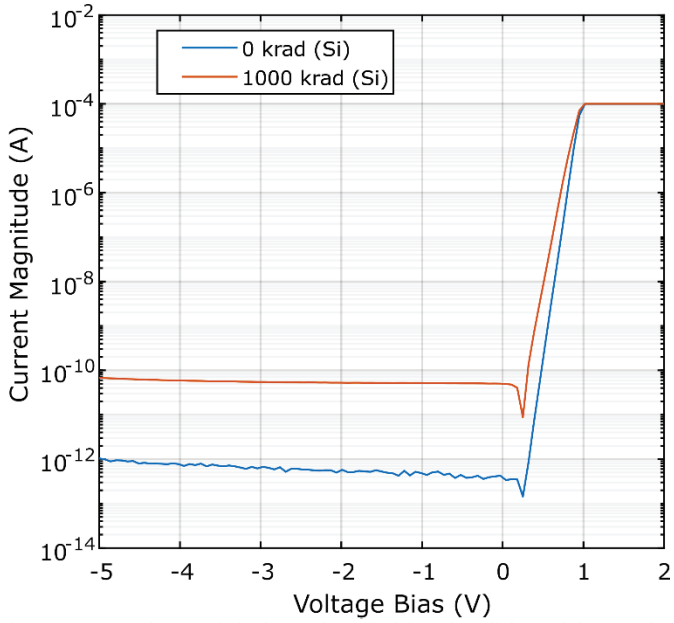

Fig. 6. DC IV characteristic for a Si vertical junction disk modulator. The mount temperature is set to 22 °C before and after irradiation at 1 Mrad (Si) ^{60}Co dose. The reverse bias current increases by a factor of ~70 and no built-in voltage shift is observed after irradiation.

As with the photodetectors, the bandwidth of the disk modulators is a key performance parameter to ensure high speed operation. The bandwidth here was measured directly with a VNA driving the modulator through port 1 and a 30 GHz photodetector receiving the signal back to port 2, yielding a scattering parameter, S_{21}.

The laser power was set to -15 dBm and TE polarization, the device was reverse biased at 2 V and a -10 dBm VNA power output was used to probe the bandwidth. We use $|S_{21}|$ and not $|S_{21}|^2$ to determine the bandwidth per common practice [36]. Rather than a lumped RC model we simply use a smoothing spline to determine the 3dB crossing frequency.

At a given temperature, voltage bias and optical polarization, there is still ambiguity about bias wavelength used in modulation. This is an important decision because it strongly affects the resulting modulation amplitude on the optical carrier. The following procedure was used to determine the optimal wavelength for determining the bandwidth: (1) RF spectra were obtained in a 1000 pm window about the center of the resonance, (2) the mean $|S_{21}|$ amplitude between 100 MHz and 1 GHz, which is flat for all observed spectra, was calculated, (3) the wavelength position of the maximum $|S_{21}|$ position was determined and (4) the smoothing spline-fit bandwidth was recorded at this position.

For the device tested in this work, the maximum amplitude is found to be 70 pm detuned from the resonance center. The bandwidth at 0 and 1 Mrad ^{60}Co gamma doses was determined. A 1 Mrad (Si) ^{60}Co dose decreases the bandwidth down to 16.6 GHz from 17.75 GHz (a 6.5 % drop).

Finally, we show high speed eye diagrams and bit error rate test (BERT) measurements for these modulators at 10 Gb/s. Here 0 dBm of laser power was used at TE polarization and 2 V reverse bias. The BERT modulation amplitude was set to 1.8 V.

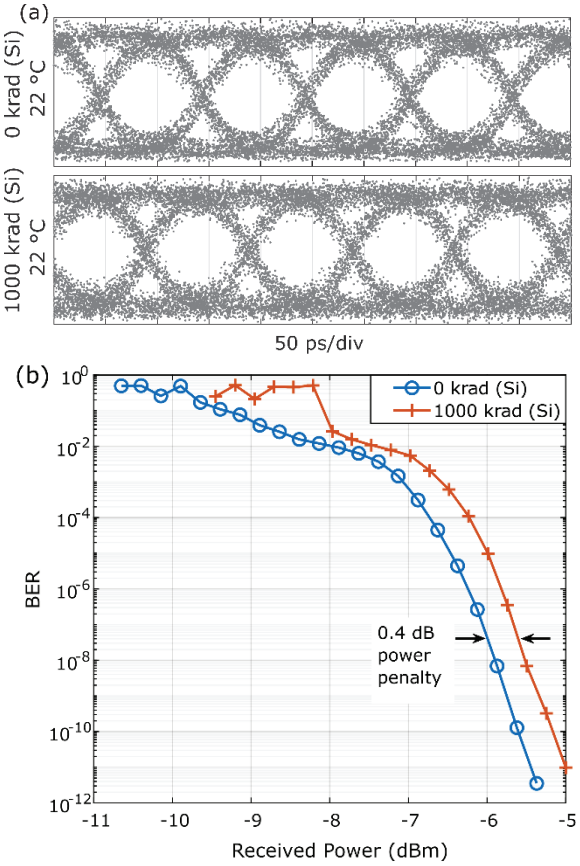

Fig. 7. (a) eye diagram and (b) BERT measurements at 10 Gb/s for a Si vertical junction disk modulator at TE polarization, 0 dBm laser power, 2 V reverse bias, 1.8 V BER amplitude and two different ^{60}Co gamma doses. A slight closing of the eye can be seen with a 1 Mrad (Si) dose in the triangular regions between eyes corresponding to a decrease of SNR with a 0.4dB power penalty.

The results for 0 krad and 1 Mrad at 22 °C are shown in Fig. 7. One can see that the eye diagram in Fig. 14a remains open and clean at both doses. There is a slight closing of the eyes with 1 Mrad exposure that can be seen most easily in the triangular regions, indicating a slight decrease in the signal to noise ratio (SNR). The observed decrease in SNR is manifested in the 0.4dB power BERT penalty shown in Fig 14b. This result is consistent with the high-speed bandwidth measurements showing the devices slowing down with gamma radiation exposure.

IV. Discussion

A key performance metric for these devices is their bandwidth. A higher bandwidth allows a given device to perform electro-optic conversion at a greater rate or for fewer electro-optic devices to be used in parallel to process a given amount of data, simplifying the system. An important question is why the Ge PIN photodiodes have a stable bandwidth after 1 Mrad whereas the Si disk diode modulators experience a 6.5 % decrease in bandwidth after the same dose. This disparity in radiation hardness can be explained in terms of the interrelation between device geometry and physics.

Gamma irradiation primarily produces positive charging effects in bulk oxide and at semiconductor-insulator interfaces [31], which can be significant enough to invert the p-doped semiconductor within the device. For the case of the Ge PIN, the device speed is determined by the transit time of the generated carriers in the center of the intrinsic Ge region, which is going to be weakly affected by charging effects near the lateral Ge-SiO_2 interfaces. The vertical-junction disk modulator however has a large p-Si/SiO_2 interface on top of the active region of the disk which is highly susceptible to attenuation of the hole carrier concentration due to top interface inversion. This alone would decrease the modulation strength due to fewer free carriers interacting with the optical mode [32], as was observed in [33].

V. Conclusion

In this work we characterized key performance parameters for waveguide-integrated Ge PIN photodiodes and Si vertical junction disk modulators from 0 up to 1 Mrad (Si) of ^{60}Co gamma radiation. Both devices saw a significant increase in reverse bias current with gamma dose. Whereas the 3dB bandwidth of the Si disk modulator was reduced by 6.5 % after 1 Mrad (Si) of gamma radiation, the Ge PIN photodiode bandwidth was not affected.

A physical explanation for the effect of gamma radiation is suggested where device geometry and physics primarily determine the degree of radiation hardness.

Acknowledgment

Sandia National Laboratories is a multi-mission laboratory managed and operated by National Technology & Engineering Solutions of Sandia, LLC, a wholly owned subsidiary of Honeywell International Inc., for the U.S. Department of Energy's National Nuclear Security Administration under contract DE-NA0003525. The views expressed in the article do not necessarily represent the views of the U.S. Department of Energy or the United States Government.

References

[1] E. Timurdogan, C. M. Sorace-Agaskar, J. Sun, E. S. Hosseini, A. Biberman, M. R. Watts, "An ultralow power athermal silicon modulator," *Nature Communications*, vol. 5, no. 4008, pp. 1-11, June 2014.

[2] A. Liu *et al*., "Wavelength Division Multiplexing Based Photonic Integrated Circuits on Silicon-on-Insulator Platform," in *IEEE Journal of Selected Topics in Quantum Electronics*, vol. 16, no. 1, pp. 23-32, Jan.-Feb. 2010.

[3] B. G. Lee, A. Biberman, P. Dong, M. Lipson and K. Bergman, "All-Optical Comb Switch for Multiwavelength Message Routing in Silicon Photonic Networks," in *IEEE Photonics Technology Letters*, vol. 20, no. 10, pp. 767-769, May15, 2008.

[4] A. L. Lentine *et al*., "Silicon photonics platform for national security applications," *2015 IEEE Aerospace Conference*, Big Sky, MT, 2015, pp. 1-9.

[5] L. Chen *et al*., "Silicon photonics for 100G-and-beyond coherent transmissions," *2016 Optical Fiber Communications Conference and Exhibition (OFC)*, Anaheim, CA, 2016, pp. 1-3. [Online]. Available: http://ieeexplore.ieee.org/abstract/document/7537288/.

[6] T. Pinguet *et al*., "25 Gb/s silicon photonic transceivers," *The 9th International Conference on Group IV Photonics (GFP)*, San Diego, CA, 2012, pp. 189-191.

[7] T. Liljeberg, "Silicon photonics and the future of optical connectivity in the data center," *2017 IEEE Optical Interconnects Conference (OI)*, Santa Fe, NM, 2017, pp. 1-2. [8] R. Grzybowski, "MACOM's Laser Integrated PIC (L-PIC) platform using Self-Aligned Etch Facet Technology (SAEFTTM) For Data Center Networks," in *Advanced Photonics 2017 (IPR, NOMA, Sensors, Networks, SPPCom, PS)*, OSA Technical Digest. [online].

[8] R. Grzybowski, "MACOM's Laser Integrated PIC (L-PIC) platform using Self-Aligned Etch Facet Technology (SAEFTTM) For Data Center Networks," in *Advanced Photonics 2017 (IPR, NOMA, Sensors, Networks, SPPCom, PS)*, OSA Technical Digest. DOI: 10.1364/NETWORKS.2017.NeW1B.4

[9] D. A. Scribner, M. R. Kruer and J. M. Killiany, "Infrared focal plane array technology," in *Proceedings of the IEEE*, vol. 79, no. 1, pp. 66-85, Jan 1991.

[10] V. S. Argabright, J. E. VanCleve, E. E. Bachtell, M. J. Hegge, S. P. McArthur, F. C. Dumont, A. C. Rudeen, J. L Pullen, D. A. Teusch, D. S. Tennant, P. D. Atcheson. (July 2008). The Kepler photometer focal plane array. Proc. SPIE 7010, Space Telescopes and Instrumentation 2008: Optical, Infrared, and Millimeter, 70102L. [Online]. Available: http://dx.doi.org/10.1117/12.789913.

[11] M. R. Watts, A. L. Lentine, D. C. Trotter, W. A. Zortman, R. W. Young, D. Campbell, and S. Shinde. (2009). Low Power Silicon Microphotonic Communications for Embedded Systems. Invited, in Proc. 13th Annual Workshop on High Performance Embedded Computing (HPEC), Lexington, MA. [Online]. Available: http://www.rle.mit.edu/pmg/documents/2009Watts-1.pdf.

[12] M. R. Watts, *et al.* (2009). Low Power Silicon Microphotonic Communications for Embedded Systems. Presented at Proc. 13th Annual Workshop on High Performance Embedded Computing (HPEC), Lexington, MA. [Online]. Available: https://www.ll.mit.edu/HPEC/agendas/proc09/Day1/F2_1445_Watts_presentation.pdf.

[13] C. Starck, "Long wavelength VCSEL with tunnel junction and metamorphic AlAs/GaAs conductive DBR," *LEOS '99. IEEE Lasers and Electro-Optics Society 1999 12th Annual Meeting*, San Francisco, CA, 1999, pp. 139-140 vol.1.

[14] C. T. DeRose, D. C. Trotter, W. A. Zortman, A. L. Starbuck, M. Fisher, M. R. Watts, and P. S. Davids, "Ultra compact 45 GHz CMOS compatible Germanium waveguide photodiode with low dark current," *Opt. Express,* vol. 19, pp. 24897-24904, 2011.

[15] A. Novack, M. Gould, Y. Yang, Z. Xuan, M. Streshinsky, Y. Liu, G. Capellini, A. E.-J. Lim, G.-Q. Lo, T. Baehr-Jones, and M. Hochberg, "Germanium photodetector with 60 GHz bandwidth using inductive gain peaking," *Opt. Express*, vol. 21, pp. 28387-28393, 2013.

[16] L. Vivien, J. Osmond, J.-M. Fédéli, D. Marris-Morini, P. Crozat, J.-F. Damlencourt, E. Cassan, Y. Lecunff, and S. Laval, "42 GHz p.i.n Germanium photodetector integrated in a silicon-on-insulator waveguide," *Opt. Express*, vol. 17, pp. 6252-6257, 2009.

[17] M. R. Watts, D. C. Trotter, R. W. Young and A. L. Lentine, "Ultralow power silicon microdisk modulators and switches," *2008 5th IEEE International Conference on Group IV Photonics*, Cardiff, 2008, pp. 4-6.

[18] Q. Xu, B. Schmidt, S. Pradhan and M. Lipson, "Micrometre-scale silicon electro-optic modulator," *Nature* vol. 435, pp. 325–327, 2005.

[19] M. R. Watts, W. A. Zortman, D. C. Trotter, R. W. Young, and A. L. Lentine, "Vertical junction silicon microdisk modulators and switches," *Opt. Express*, vol. 19, pp. 21989-22003, 2011.

[20] P. Dong, R. Shafiiha, S. Liao, H. Liang, N.-N. Feng, D. Feng, G. Li, X. Zheng, A. V. Krishnamoorthy, and M. Asghari, "Wavelength-tunable silicon microring modulator," *Opt. Express*, vol. 18, pp. 10941-10946, 2010.

[21] G. T. Reed, G. Mashanovich, F. Y. Gardes, D. J. Thomson, "Silicon optical modulators," *Nature Photonics*, vol. 4, pp. 518–526, 2010.

[22] E. G. Stassinopoulos and J. P. Raymond, "The space radiation environment for electronics," in *Proceedings of the IEEE*, vol. 76, no. 11, pp. 1423-1442, Nov 1988.

[23] J. R. Schwank, M. R. Shaneyfelt and P. E. Dodd, "Radiation Hardness Assurance Testing of Microelectronic Devices and Integrated Circuits: Radiation Environments, Physical Mechanisms, and Foundations for Hardness Assurance," in *IEEE Transactions on Nuclear Science*, vol. 60, no. 3, pp. 2074-2100, June 2013.

[24] R. L. Pease, A. H. Johnston and J. L. Azarewicz, "Radiation testing of semiconductor devices for space electronics," in *Proceedings of the IEEE*, vol. 76, no. 11, pp. 1510-1526, Nov 1988.

[25] M. Van Uffelen, J. Mols, A. Goussarov, C. Neumeyr, M. Ortsiefer and F. Berghmans, "Comparison of gamma and proton-induced radiation damage in long-wavelength VCSELs," *2007 9th European Conference on Radiation and Its Effects on Components and Systems*, Deauville, 2007, pp. 1-4.

[26] F. Berghmans, B. Brichard, A. F. Fernandez and M. Van Uffelen, "Reliability issues for optical fibre technology in nuclear applications," *Proceedings of 2003 5th International Conference on Transparent Optical Networks, 2003.*, 2003, pp. 252-257 vol.1.

[27] P. Leroux, W. De Cock, M. Van Uffelen and M. Steyaert, "Design and Radiation Assessment of Optoelectronic Transceiver Circuits for ITER," in: Topical Workshop on Electronics for Particle Physics, Naxos, Greece, Sep. 2008, pp.167-171 (CERN-2008-008).

[28] S. Seif, El Nasr-Storey, *et al*., "Modeling TID Effects in Mach-Zehnder Interferometer Silicon Modulator for HL-LHC Data Transmission Applications," in *IEEE Transactions on Nuclear Science*, vol. 62, no. 6, pp. 2971-2978, Dec. 2015.

[29] J. Wright, D. C. Trotter, W. Zortman, A. L. Lentine, E. Shaner, M. R. Watts, A. Akturk, and M. Peckerar. (2012). Cryogenic Operation of Silicon Photonic Modulators. In *Advanced Photonics Congress, OSA Technical Digest*, paper IM2A.5. [Online]. Available: https://doi.org/10.1364/IPRSN.2012.IM2A.5.

[30] Michael Gehl, Christopher Long, Doug Trotter, Andrew Starbuck, Andrew Pomerene, Jeremy B. Wright, Seth Melgaard, John Siirola, Anthony L. Lentine, and Christopher DeRose, "Operation of high-speed silicon photonic micro-disk modulators at cryogenic temperatures," *Optica*, vol. 4, pp. 374-382, 2017.

[31] H. N. Becker and A. H. Johnston, "Dark current degradation of near infrared avalanche photodiodes from proton irradiation," in *IEEE Transactions on Nuclear Science*, vol. 51, no. 6, pp. 3572-3578, Dec. 2004.

[32] R. Soref and B. Bennett, "Electrooptical effects in silicon," in *IEEE Journal of Quantum Electronics*, vol. 23, no. 1, pp. 123-129, January 1987.

[33] E. H. Snow, A. S. Grove and D. J. Fitzgerald, "Effects of ionizing radiation on oxidized silicon surfaces and planar devices," in *Proceedings of the IEEE*, vol. 55, no. 7, pp. 1168-1185, July 1967.